Dependence of Rydberg-Atom Optical Lattices on the Angular Wave Function

S. E. Anderson and G. Raithel

Phys. Rev. Lett. **109**, 023001 — Published 10 July 2012

DOI: 10.1103/PhysRevLett.109.023001

Dependence of Rydberg-atom optical lattices on the angular wavefunction

S. E. Anderson* and G. Raithel
Department of Physics, University of Michigan, Ann Arbor, MI 48109
(Dated: May 15, 2012)

We investigate the dependence of optical-lattice trapping potentials for Rydberg atoms on the angular portion of the atomic wavefunction. While ground-state atoms are point-like in relation to an optical-lattice field, Rydberg-atom wavefunctions extend over a substantial fraction of the lattice period, which leads to a dependence of the lattice trapping potential on the angular portion of the spatial wavefunction. The angular dependence of the potential is measured using various (j, m_j) levels of ^{85}Rb Rydberg nD states ($50 \leq n \leq 65$) prepared in a one-dimensional optical lattice (wavelength 1064 nm) and a transverse DC electric field. The measured optical lattice depths are found to be in agreement with theoretical results.

PACS numbers: 37.10.Jk, 32.80.Ee

In optical lattices, the dependence of the optical potentials on the magnetic quantum number, m, is of fundamental importance. For ground-state atoms, this dependence has been well known since the late 1980s [1, 2] and has been widely exploited in laser cooling experiments, for example in achieving sub-Doppler temperatures through the mechanism of Sisyphus cooling [3]. In optical lattices for Rydberg atoms, an analogous dependence of the trapping potentials on the m quantum number has not been previously observed. The m-dependence of the lattice potentials affects both the trapping behavior as well as lattice-induced shifts of electromagnetic transitions of the atoms in the lattice. The tunability of the Rydberg-atom trapping potentials using the angular degrees of freedom will be important for applications of Rydberg-atom optical lattices. For instance, in quantum computing applications of such lattices [4], it is desired to tailor the lattice in such a way that lattice-induced shifts of ground- to Rydberg-state transitions are minimized. In high precision spectroscopy applications [5], it will be beneficial to minimize the lattice-induced shifts of microwave transitions between selected Rydberg levels.

The trapping potential for Rydberg atoms in an optical lattice arises from a ponderomotive force, akin to the trapping force present in Paul ion traps [6]. In a laser field with electric-field amplitude E and angular frequency ω, the quasi-free Rydberg electron experiences an energy shift given by the free-electron ponderomotive energy, $V_\mathrm{p} = e^2E^2/(4m_\mathrm{e}\omega^2)$ [7], where e is the elementary charge and m_e the electron mass. In an optical lattice, V_p represents a periodically modulated perturbation potential acting on the Rydberg electron. The entire atom can be trapped due to this potential since the ionic Rydberg-atom core is weakly bound to the Rydberg electron. The adiabatic trapping potential for the center-of-mass of the Rydberg atom is given by [8]

$$V_\mathrm{ad}(\mathbf{R}) = \int d^3r V_\mathrm{p}(\mathbf{r}+\mathbf{R})\,|\psi(\mathbf{r})|^2, \qquad (1)$$

where $\mathbf{R}$ is the center-of-mass coordinate of the atom, $\mathbf{r}$ is the relative coordinate of the Rydberg electron, $V_\mathrm{p}(\mathbf{r}+\mathbf{R})$ is the position-dependent free-electron ponderomotive energy, and $\psi(\mathbf{r})$ is the Rydberg electron's probability distribution. Therefore, V_ad is a spatial average of the free-electron ponderomotive energy weighted by the Rydberg electron's probability distribution [8]. Since the Rydberg-atom wavefunction covers a substantial fraction of the lattice period, the V_ad depend on all quantum numbers (n, l, j, m_j). In previous work, the dependence of the adiabatic trapping potentials of the ponderomotive optical lattice (POL) on the principal quantum number, n, has been experimentally demonstrated using various Rydberg nS states (which do not exhibit angular substructure) [9].

The lattice potentials for atoms in low-lying or in Rydberg states are generally expected to depend on (j, m_j); however, the reasons for that dependence are quite different in the two cases. For atoms in low-lying states, the lattice potential arises from an AC electric dipole moment between bound atomic states, and the (j, m_j)-dependence reflects the Clebsch-Gordan coefficients in the atom-field interaction [10]. This leads to intensity- and polarization-dependent trapping potentials. In contrast, for Rydberg atoms in POLs, the trapping results from the free-electron polarizability. Since the size of the Rydberg wavefunctions is on the same order as the lattice period, the angular portion of the Rydberg wavefunction can have a dramatic effect on the averaging in Eq. 1, resulting in a (j, m_j)-dependence of the adiabatic potentials. States having wavefunctions that mostly extend in the plane transverse to the lattice axis will experience more deeply modulated lattice potentials than those elongated in the direction of the lattice axis. The adiabatic potentials obtained from Eq. 1 depend on light intensity but not on polarization. In the present work, we demonstrate the dependence of the lattice trapping potentials on the angular portion of the Rydberg wavefunction by measuring the POL depth for several (j, m_j) sublevels of Rydberg nD states.

In the experimental setup, ^{85}Rb atoms are loaded

into a magneto-optical trap (MOT) with a temperature ∼200 μK. The one-dimensional lattice is established by focusing a 1064 nm beam into the MOT [power of 1 W, full-width at half maximum of the intensity profile (FWHM) of 13 μm], retro-reflecting and refocusing it. The lattice is always on. The MOT and repumper beams are turned off during Rydberg excitation and detection. Ground-state atoms in the lattice are transferred to Rydberg states via two photon excitation (excitation pulse duration 0.5 μs). The lower-transition laser (FWHM 150 μm) has a wavelength of 780 nm, is ≈1.2 GHz detuned from the $5P_{3/2}$ intermediate state, and is collinear with the lattice beams. The upper-transition laser has a wavelength of ≈480 nm (FWHM ∼15 μm), is tuned into two-photon resonance with the $5S \rightarrow nD$ transition, and forms an angle of about 45° with all other laser beams. The number of Rydberg atoms produced is measured by ionizing them with a ramped electric field and detecting the freed electrons with a micro-channel plate [11]. The number of Rydberg atoms per cycle is about one, so that Rydberg-atom interactions are not important. With the lattice off, the observed FWHM of the Rydberg excitation lines are between 2-3 MHz, which is just slightly above the width of the power spectrum of a square pulse with 0.5 μs duration. Using the known beam powers, beam profiles, intermediate state detuning, and $5P$-Rydberg transition matrix elements, we estimate two-photon Rabi frequencies up to $2\pi \times 500$ kHz. Hence, for our excitation pulse duration transition broadening due to saturation plays no significant role. We attribute the slight broadening of the lattice-free Rydberg excitation lines to electric field inhomogeneities and the MOT magnetic field.

In order to investigate the lattice potentials for the (j, m_j) sublevels of Rydberg nD states individually, it is necessary to lift degeneracies. We therefore apply a DC electric field. For technical reasons, the DC field is oriented in the direction transverse to the axis of the lattice. With the DC field applied, the Stark effect is the dominant perturbation, with a quantization axis transverse to the lattice beams. The Rydberg-atom lattice potential varies in depth for the five Stark substates of the $nD_{3/2}$ and $nD_{5/2}$ levels.

Figure 1 shows the spectrum of the $50D$ Rydberg level in both the lattice and a transverse electric field of 1.6 V/cm, obtained by scanning the frequency of the upper transition excitation laser. The $50D_{3/2}$ and $50D_{5/2}$ levels split into a total of five components, labeled in Fig. 1 in order of increasing energy. In the limit of small DC field, the five components connect with the following levels: (1) $50D_{3/2}$ $|m_j|$=3/2, (2) $50D_{5/2}$ $|m_j|$=5/2, (3) $50D_{3/2}$ $|m_j|$=1/2, (4) $50D_{5/2}$ $|m_j|$=3/2, and (5) $50D_{5/2}$ $|m_j|$=1/2. The large peaks for each component are signal from atoms outside of the lattice (red solid arrows in Fig. 1), while the blue-shifted triangular structures reflect the shifts of the optical transition frequency due to the lattice trapping potentials. Since the atoms are laser-cooled near the bottoms of the $5S$ lattice wells, the lattice-induced structures in the spectrum exhibit a sharp cutoff on the high frequency side (dashed arrows in Fig. 1).

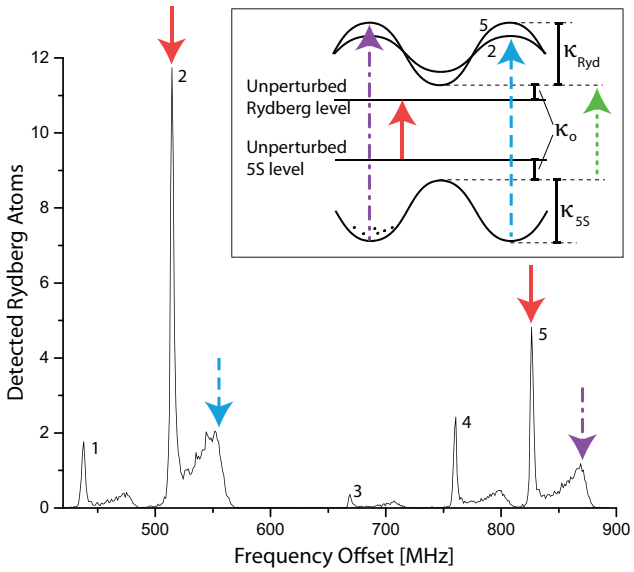

FIG. 1. (Color online.) Optical excitation spectrum of the $50D$ Rydberg level in the lattice and a transverse DC electric field. The Stark components, labeled 1-5, exhibit structures on the high-frequency side that reflect lattice-induced shifts of the optical transitions. Inset: Ground and Rydberg levels in the lattice. The arrows indicate how the maxima in the experimental spectrum correlate with the shapes of the lattice potentials.

The blue-shifted structures in the spectrum shown in Fig. 1 yield information on the depth of the Rydberg lattice for each Stark level. The maximum lattice-induced shift consists of the ground-state modulation depth (κ_{5S} in the inset of Fig. 1), the Rydberg-state modulation depth (κ_{Ryd}), and an offset (κ_o). The offset can arise from an imbalance of the intensities of the lattice beams, leading to a reduced lattice intensity modulation depth. There also is a contribution to κ_o from the intrinsic averaging in Eq. 1. Due to the averaging, the value of κ_o does not reach zero even in a perfectly modulated lattice. Here, we are interested in how κ_{Ryd} depends on the angular structure of the five Stark levels. The inset of Fig. 1 shows that κ_{Ryd} can be obtained by subtracting κ_o and κ_{5S} from the measured maximum lattice-induced shift. The ground-state lattice depth, κ_{5S}, is fixed. For an independent measurement of κ_o, we invert the lattice potential immediately before Rydberg excitation using an electro-optic technique [12]. Following the lattice inversion, the ground-state atoms are located near maxima in the ground-state potential. Before they move away, they are excited to minima of the Rydberg-state potential (green dotted arrow in the inset of Fig. 1 and correspond-

ing curve in Fig. 2). Measurement of the lattice-induced shift in the inverted lattice case yields κ_o.

In the experimental spectra, signal from atoms outside of the lattice (solid red arrows in Fig. 1) tends to overwhelm the desired signal from the atoms inside the lattice. To address this issue, we apply a "dumper" pulse between the turnoff of the MOT laser beams and the application of the excitation pulses. The dumper pulse has a duration of 25 μs and is resonant with the $5S_{1/2}$, F=3 $\rightarrow$ $5P_{3/2}$, F'=2 transition. The dumper optically pumps atoms outside of the lattice into the F=2 ground-state. Following the dumper pulse, only the F=3 atoms left in the lattice are accessible for optical excitation to the Rydberg state, resulting in a cleaner spectrum of the lattice-induced shifts.

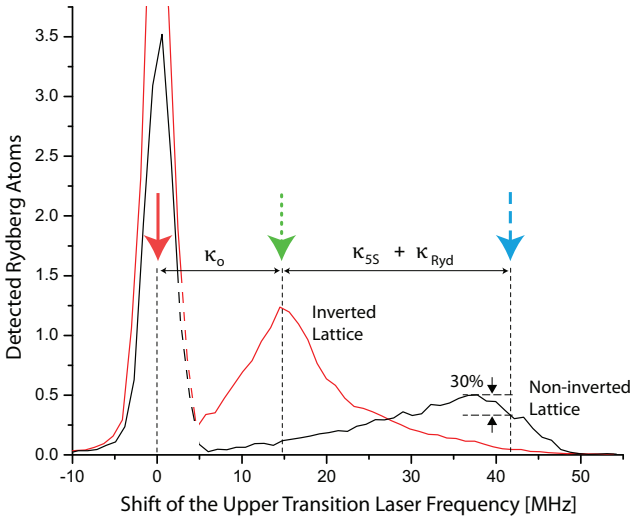

FIG. 2. (Color online.) Optical excitation spectra for level 2 of Fig. 1 in a transverse DC field and a non-inverted lattice and inverted lattice. Spectral features, indicated by arrows, enable a measurement of the Rydberg-state lattice depth ($\kappa_{\rm Ryd}$).

In Fig. 2 we show typical optical excitation spectra of level 2 from Fig. 1 for the two cases of an inverted and a non-inverted lattice. The dumper is engaged to the right of the dashed segments in the data in Fig. 2, leaving the unshifted signal as a frequency reference (the large peak at 0 MHz). Figure 2 clearly shows that the peak in the inverted-lattice spectrum is shifted from that in the case of the non-inverted lattice. As indicated in the figure, we use the peak positions to determine the shifts κ_o and $\kappa_o + \kappa_{5S} + \kappa_{\rm Ryd}$.

To extract $\kappa_{\rm Ryd}$ from the spectra, one must consider exactly how the experimentally observed peaks in the lattice-induced features are related to the various values of κ. For the inverted lattice, the ground-state atoms are located near a saddle point of the lightshift potentials, which results from mismatched spot sizes of the two lattice beams. In the utilized experimental setup, there is an unavoidable mismatch. The corresponding peak in the excitation spectrum (green dotted arrow in Fig. 2) is broadened both to the low- and high-frequency sides, due to atoms that are displaced from the saddle point radially and longitudinally relative to the lattice axis, respectively. Due to the balanced broadening, the peak center gives an accurate reading for κ_o. In contrast, for the non-inverted lattice the ground-state atoms are located near a three-dimensional intensity maximum, not a saddle point. Therefore, any thermal spread of the atoms away from the intensity maximum causes a shift of the Rydberg-atom excitation frequency to lower frequencies. Hence, in the non-inverted lattice the excitation spectrum is only broadened to the low frequency side, and the peak in the spectrum is shifted toward lower frequency. To obtain a quantitative estimate for how far the peak is shifted, we have simulated the excitation spectrum for temperatures ranging from 100-300 μK for lightshift potentials that correspond to our experiment. The simulated spectra show that the frequency corresponding to a one-third drop in signal from the peak (blue dashed arrow in Fig. 2) approximates the value of $\kappa_o + \kappa_{5S} + \kappa_{\rm Ryd}$ to within $\pm$1 MHz. The procedure is indicated in Fig. 2. With this reading, the reading for κ_o, and the fixed value of κ_{5S}, the Rydberg lattice depth $\kappa_{\rm Ryd}$ is obtained. To investigate the angular dependence of the POL potentials, we repeat the procedure explained in Fig. 2 for several other nD and (j, $|m_j|$) levels. The measurement results are listed in Table I.

TABLE I. POL Depth Measurement Results

Level	Measured $\kappa_{\rm Ryd}$ (MHz)	Label
$65D_{5/2}$ $\lvert m_j\rvert$=5/2	-4.1$\pm$3	A
$55D_{5/2}$ $\lvert m_j\rvert$=5/2	1.4$\pm$3	B
$50D_{5/2}$ $\lvert m_j\rvert$=5/2	4.5$\pm$3	C
$65D_{5/2}$ $\lvert m_j\rvert$=1/2	1.1$\pm$3	D
$55D_{5/2}$ $\lvert m_j\rvert$=1/2	10.0$\pm$3	E
$50D_{5/2}$ $\lvert m_j\rvert$=1/2	9.5$\pm$3	F

We find that the values of $\kappa_{\rm Ryd}$ clearly vary from state to state, demonstrating the angular dependence of the Rydberg lattice depth. We compare our measured results with calculated $\kappa_{\rm Ryd}$ values for the cases studied in the experiment. In the calculation, the depth of the Rydberg adiabatic potentials was obtained by numerical diagonalization of the Rydberg atoms' internal-state Hamiltonian at the light-field maxima and minima. The lattice depth for a given Rydberg level is given by the difference between that level's energy at these two locations. It is noted that the computation requires large Rydberg-state basis sets, since the system does not have any continuous symmetry in crossed electric and lattice-induced fields.

In Fig. 3, the experimental measurements of $\kappa_{\rm Ryd}$ are plotted against the calculated values. The data follow the

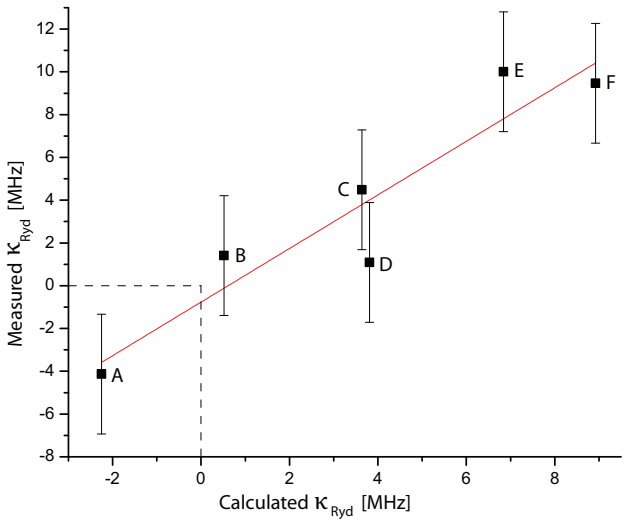

FIG. 3. Symbols: Measured vs. calculated POL potential depths for the levels listed in Table I. The error bars reflect systematic and measurement uncertainties. Line: A linear fit to the data points.

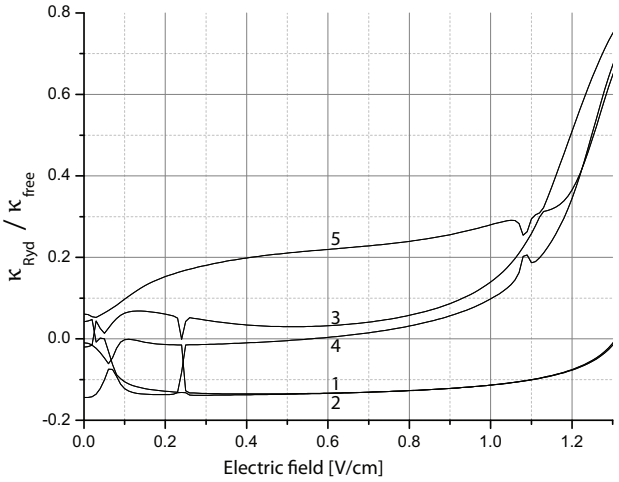

FIG. 4. Calculated depth of the $65D$ POL potentials, $\kappa_{\rm Ryd}$, in units of the free-electron POL depth, $\kappa_{\rm free}$, for various Stark levels as a function of DC field. The level labeling follows the scheme used in Fig. 1. Negative POL depths correspond to cases in which the Rydberg-atom center-of-mass is attracted to intensity maxima in the lattice.

expected trend, as the linear fit to the data has a slope of one and passes through the origin within the bounds of the fitting uncertainty. The error bars in Fig. 3 reflect the measurement and systematic uncertainties associated with the data.

The measurement uncertainty is ± 1 MHz and mostly arises from the uncertainty associated with measuring the lattice-induced shift in the non-inverted lattice, as described above. Systematic error sources include daily variations in optical lattice alignment. Comparing day-to-day results, we estimate an alignment-induced uncertainty of ≈ 2 MHz. The excitation laser is locked to a tunable Fabry Perot (FP), and a source of systematic error is also thermal drift of the FP. Monitoring the count rate as a function of time with the laser initially set to the peak of a Rydberg excitation line of known width, we found a thermal drift uncertainty of ≈ 1 MHz. Nonlinearity in the FP mechanical tracking (the experimental method used to scan the laser across the spectrum) also adds to the systematic error. By scanning the laser repeatedly over a fixed frequency range, we found a mechanical tracking uncertainty of $\lesssim 2$ MHz.

In order to obtain further insight into the angular dependence of the POL potentials and to interpret the measured negative values of $\kappa_{\rm Ryd}$, we calculated $\kappa_{\rm Ryd}$ for (j, $m_{\rm j}$) levels of nD states as a function of DC field. The result for $65D$ is shown in Fig. 4 (curve labels correspond to the ones in Fig. 1). For DC field values $\lesssim 0.05$ V/cm, the fine structure is dominant and the DC field provides a small perturbation. For DC field values $\gtrsim 0.1$ V/cm, the DC field effects dominate the fine structure; however, the DC field is still weak enough to largely avoid mixing of the D states with neighboring P and F states. Between the fine-structure- and the electric-field-dominant regimes, the angular wavefunctions rearrange, causing a reshuffling of the curves around 0.07 V/cm in Fig. 4. The structures in the curves near 0.25 V/cm and 1.1 V/cm are due to crossings of Stark states in the electric-field-dominant regime. For states with negative $\kappa_{\rm Ryd}$, the extent of the Rydberg wavefunction along the lattice axis approximately equals the lattice period. While the center-of-mass of the atom is located at an intensity maximum, the lobes of the electronic probability distribution are located at adjacent intensity minima, where they experience a minimal ponderomotive energy. The Rydberg center-of-mass is attracted to the lattice intensity maximum located between the wavefunction lobes. In this case, the minima of the adiabatic Rydberg-atom trapping potential are co-located with the minima of the ground-state potential. This condition will be desirable in applications because it allows for straightforward preparation of trapped Rydberg atoms from red-detuned optical traps for ground-state atoms. The ability to shape the Rydberg-atom potentials using the angular structure of the wavefunction blends into work performed elsewhere, in which magic-wavelength optical lattices for Rydberg atoms are pursued [13].

We have provided an experimental demonstration of the angular dependence of the POL potentials for Rydberg atoms. Lattice depths for (j, $m_{\rm j}$) sublevels of $nD_{5/2}$ states were measured and found to vary substantially in magnitude. We have also demonstrated that certain aspect ratios of atom size to lattice period result in Rydberg lattice potential depths that are sign-matched with the

ground-state potential depths. In future work, we consider the preparation of highly elongated Stark states in the optical lattice using larger DC fields. Such states have essentially one-dimensional atomic wavefunctions oriented in the direction of the transverse field, leading to very deep trapping potentials. Since they also have large permanent electric dipole moments, such a system could provide a platform to study strong interactions and many-body effects in systems of optically trapped Rydberg atoms.

S.E.A. acknowledges support from DOE SCGF. This work was supported by NSF Grants No. PHY-0855871 and No. PHY-0114336.

*andsare@umich.edu

[1] J. Dalibard and C. Cohen-Tannoudji, J. Opt. Soc. Am. B **6**, 2023 (1989).

[2] P. J. Ungar, D. S. Weiss, E. Riis, and S. Chu, J. Opt. Soc. Am. B **6**, 2058 (1989).

[3] H. J. Metcalf and P. van der Straten, *Laser Cooling and Trapping* (Springer, New York, 1999), and references therein.

[4] M. Saffman, T. G. Walker and K. Mølmer, Rev. Mod. Phys. **82**, 2313 (2010).

[5] B. Knuffman and G. Raithel, Phys. Rev. A **75**, 053401 (2007).

[6] W. Paul, Rev. Mod. Phys. **62**, 531 (1990).

[7] S. H. Friedrich, *Theoretical Atomic Physics* (Springer, Berlin, 2004).

[8] S. K. Dutta, J. R. Guest, D. Feldbaum, A. Walz-Flannigan, and G. Raithel, Phys. Rev. Lett. **85**, 5551 (2000).

[9] K. C. Younge, B. Knuffman, S. E. Anderson, and G. Raithel, Phys. Rev. Lett. **104**, 173001 (2010).

[10] P. S. Jessen and I. H. Deutsch, Adv. At. Mol. Phys. **37**, 95 (1996).

[11] T. F. Gallagher, *Rydberg Atoms* (Cambridge University Press, Cambridge, U.K., 1994).

[12] S. E. Anderson, K. C. Younge, and G. Raithel, Phys. Rev. Lett. **107**, 263001 (2011).

[13] S. Zhang, F. Robicheaux, and M. Saffman, Phys. Rev. A **84**, 043408 (2011).